and so a wide range of "connection strengths" is accessible. The technique is not limited to a single pair of nodes. In theory, a large number of nodes could be connected in common, with varying connection strengths again determined by the conductivity between each node and the common pool. Because the conductivity of conducting polymers can range over eight orders of magnitude, the polymer networks can store a large amount of information in a relatively small volume. A link formed by electropolymerization can be made to "forget" if the potential of all of its nodes is held negative of the polymer doping potential while the array is immersed in an electrolyte solution. We have observed that under these conditions, the polymer link undopes and becomes insulating, as expected from established polythiophene electrochemistry (20, 21). The link can be "reminded" again if the array potential is adjusted positive of the doping potential. This doping-undoping electrochemistry is a way of storing information in the form of a conductivity value. Although this method may be an advantage relative to current 2D optical or magnetic storage devices, the polymer doping process relies on ion migration and so is expected to be inherently slower than devices that use electron transport processes (such as conventional Si-based random-access memory chips).

REFERENCES AND NOTES

1. W.-J. Sah, S.-C. Lee, H.-K. Tsai, J.-H. Chen, *Appl. Phys. Lett.* **56**, 2539 (1990).
2. M. A. Sivilotti, M. R. Emerling, C. A. Mead, *AIP Conf. Proc.* **151**, 408 (1986).
3. J. J. Hopfield, J. N. Onuchic, D. N. Beratan, *J. Phys. Chem.* **93**, 6350 (1989).
4. H. P. Graf *et al.*, *AIP Conf. Proc.* **151**, 182 (1986).
5. J. Alspector, *IEEE Commun. Mag.* **11**, 29 (1989).
6. D. Psaltis, D. Brady, X.-G. Gu, S. Lin, *Nature* **343**, 325 (1990).
7. S. W. Kuffler and J. G. Nichols, *From Neuron to Brain* (Sinauer, Sunderland, MA, 1976), p. 7.
8. T. Nordstrom and B. Svensson, *J. Parallel Distrib. Comput.* **14**, 260 (1992).
9. S. Li, C. W. Macosko, H. S. White, *Science* **259**, 957 (1993).
10. J. H. Kaufman, C. K. Baker, A. I. Nazzal, M. Flickner, O. R. Melroy, *Phys. Rev. Lett.* **56**, 1932 (1986).
11. R. J. v. Gutfeld and D. R. Vigliotti, *Appl. Phys. Lett.* **56**, 2584 (1990).
12. T. Kawai, H. Motobayashi, T. Kuwabara, K. Yoshino, *Jpn. J. Appl. Phys.* **30**, L622 (1991).
13. J. J. Hickman *et al.*, *J. Am. Chem. Soc.* **111**, 7271 (1989).
14. J. J. Hickman *et al.*, *Langmuir* **8**, 357 (1992).
15. C. H. McCoy and M. S. Wrighton, *Chem. Mater.* **5**, 914 (1993).
16. G. P. Kittlesen, H. S. White, M. S. Wrighton, *J. Am. Chem. Soc.* **106**, 7389 (1984).
17. D. F. Shriver and M. A. Drezdzon, *The Manipulation of Air-Sensitive Compounds* (Wiley, New York, ed. 2, 1986), pp. 90–91.
18. A. J. Bard and L. R. Faulkner, *Electrochemical Methods* (Wiley, New York, 1980), p. 301.
19. G. Tourillon, *Handbook of Conducting Polymers*, T. A. Skotheim, Ed. (Dekker, New York, 1986), vol. 1, pp. 293–350.
20. K. Kaneto, K. Yoshino, Y. Inuishi, *Solid State Commun.* **46**, 389 (1983).
21. G. Tourillon and F. Garnier, *J. Phys. Chem.* **87**, 2289 (1983).
22. T. F. Otero and E. d. Larreta-Azelain, *Polymer* **29**, 1522 (1988).
23. H. O. Finklea and R. S. Vithanage, *J. Electroanal. Chem.* **161**, 283 (1984).

24. We thank P. Asbeck for helpful discussions and the U.S. Department of Education for a Graduate Assistance in Areas of National Need Graduate Fellowship (C.L.C.). Supported in part by an Office of Naval Research grant and by the Donors of the Petroleum Research Fund.

10 August 1993; accepted 3 November 1993

Stable Isotope Enrichment in Paleowaters of the Southeast Atlantic Coastal Plain, United States

L. Niel Plummer

Paleowaters from the Floridan aquifer system in the southeastern Atlantic coastal plain have higher D/H and $^{18}O/^{16}O$ ratios than local Holocene ground water. Maximum $\delta^{18}O$ enrichments in ground water having adjusted radiocarbon ages of 20,000 to 26,000 years are 0.7 to 2.3 per mil. The trend in isotopic enrichment in paleowaters is the reverse of that normally observed in continental glacial age ground water. Dissolved nitrogen and argon concentrations indicate, however, that the average recharge temperature was 5.3°C cooler than that today. The data indicate cool conditions in the southeast Atlantic coastal plain during the last glacial maximum, with recharge limited primarily to late summer tropical cyclones and hurricanes.

Ground water recharged during the last glacial maximum (LGM) is recognized worldwide by depletion in D and ^{18}O in comparison to Holocene ground water (1–5). This is attributed to isotopic fractionation as atmospheric moisture condenses in colder climates and, in some cases, to recharge from melting ice (6). For example, isotopically depleted paleowaters recharged during the LGM in central Europe indicate that temperatures were 7°C less than in Holocene times (3). Noble gas measurements (7) support the stable isotope data and are consistent with values of the stable isotope temperature coefficient, $\Delta\delta^{18}O/\Delta T$, of 0.40 to 0.70 per mil per degree Celsius (4, 7–9).

Studies of stable isotope depletion in European paleowaters have found no evidence that the continental temperature gradient differed between modern and glacial times (3). Therefore, it has been assumed that water vapor transport patterns over Europe were little changed in the last ice age and that the average degree of rain out of air masses was similar to the present (3).

In the southwest and south-central United States, stable isotope depletion and noble gas measurements in paleowaters indicate that temperatures were 5° to 7°C less than those in the late Wisconsin (5, 10–12). Pollen studies and other fossil records in the southeast United States also indicate a cooling of 5° to 7°C during the LGM (13, 14). In contrast, climate model results (15–18) indicate a cooling of only a few degrees in both January and July temperatures in the Gulf of Mexico surface waters at the LGM. Both model predictions (15–17) and pollen records from lake sediments (19) indicate significantly dryer conditions in the southeast United States during the LGM.

This report describes isotopically enriched paleowaters in the Floridan aquifer system of the southeast Atlantic coastal plain, United States, and compares these data with paleorecharge temperatures determined from measurements of dissolved gases. Together, these data can be used to evaluate climatic conditions and atmospheric circulation patterns in the southeastern United States during the LGM (20).

The hydrology and chemistry of the Floridan aquifer system has been extensively studied (21–23). In north-central Georgia, the aquifer system crops out as thin sand and marl of Tertiary age that thicken into limestone and dolostone to the southeast and east. The aquifer system is 600 m, and locally 800 m, thick along the Atlantic coast. The Floridan aquifer system is locally subdivided into two permeable zones, the Upper and Lower Floridan aquifers, separated by a dolomite. The Upper Floridan aquifer is typically 90 to 180 m thick in Georgia and is overlain by 90 to 180 m of low-permeability Miocene sediment, which forms the upper confining unit.

The Floridan aquifer system is underlain by Cretaceous and Tertiary clastic sedimentary rocks that generally thicken to the southeast. In Georgia, these underlying rocks are subdivided into three regional aquifers separated by confining units (24). The uppermost clastic regional aquifer (A2, or Gordon aquifer) is hydraulically con-

U.S. Geological Survey, Reston, VA 22092.

nected to the Lower Floridan aquifer in southeast Georgia. In central Georgia, the Gulf Trough graben crosses the Floridan and adjacent aquifers (Fig. 1).

Hydraulic conductivities in the Upper Floridan aquifer along the axis of the Gulf Trough are generally less than 15 m day^{-1} and typically 10- to 100-fold less than hydraulic conductivities elsewhere in the Upper Floridan aquifer. Simulations of the modern (before development) aquifer indicate that ground water reaches the Upper Floridan aquifer in southeast Georgia by horizontal flow through the Gulf Trough graben, by diffuse upward leakage from the Lower Floridan, and by downward leakage from the upper confining unit. The leakage coefficient of the upper confining unit is extremely low (less than 0.08 cm year^{-1} m^{-1}) throughout most of southeast Georgia (*23*). Toward the Atlantic coast, the Upper Floridan aquifer discharges to the upper confining unit.

Adjusted radiocarbon ages in the Upper Floridan aquifer are in excess of 20 ka (thousand years) and are in agreement with simple calculations of Darcy's law for representative hydraulic properties (*25*), which indicate travel times from the Gulf Trough to the Atlantic coast of 10 to 40 ka. Hydrologic conditions in the aquifer at 20 to 30 ka are unknown. However, it is expected that lowered sea level (*26, 27*) during the LGM resulted in lower heads in all the Coastal Plain aquifers but that the lowering of heads was greater nearer the coast and in the surficial aquifer and upper confining unit above the Upper Floridan aquifer than in deeper aquifers. Therefore, during the LGM, the Upper Floridan aquifer probably was recharged more so from diffuse upward leakage and horizontal flow through the Gulf Trough and less so from downward leakage from the upper confining unit. Increases in dissolved chloride in paleowaters downgradient of the Gulf Trough (Fig. 1) may record more diffuse upward leakage during the LGM (*28*). Sea level at the LGM was about 120 to 130 m lower than today (*26*). Calculations for the increased gradient accompanying, for example, a 100-m lowering of sea level suggest that the flow velocities were increased sixfold. Paleowaters currently found in the Upper Floridan aquifer in southeast-Georgia downgradient of the Gulf Trough are thought to represent waters that were partially trapped as sea level rose during the last deglaciation and flow velocities decreased in response to a decrease in hydraulic gradient.

We analyzed the chemistry and isotopic composition of the Upper Floridan aquifer along three flow paths in the recharge areas and downgradient in the most confined portions of the aquifer in southeast Georgia (Fig. 1). The D/H and $^{18}O/^{16}O$ ratios (*29*) of recent ground waters from recharge zones in southeast Georgia [^{14}C content is typically >50% modern ^{14}C (pmc)], and Holocene ground waters (^{14}C content of 10 to 50 pmc) are similar to the isotopic compositions of winter-spring precipitation in south-central Georgia (*30, 31*) and plot parallel to the global meteoric water line (GMWL) with a deuterium excess (d_{excess}) between 10 and 13 per mil (Fig. 2). The similarity of isotopic composition of recent and Holocene ground water to that of present-day late winter-spring precipitation is consistent with the conclusion that predominant recharge to the Upper Floridan aquifer occurs today during the late winter and spring.

The stable isotope ratios in the paleowaters progressively increase with distance down the hydraulic gradient (Fig. 3). Similar increases are seen in all three flow paths from the recharge area to about 100 km

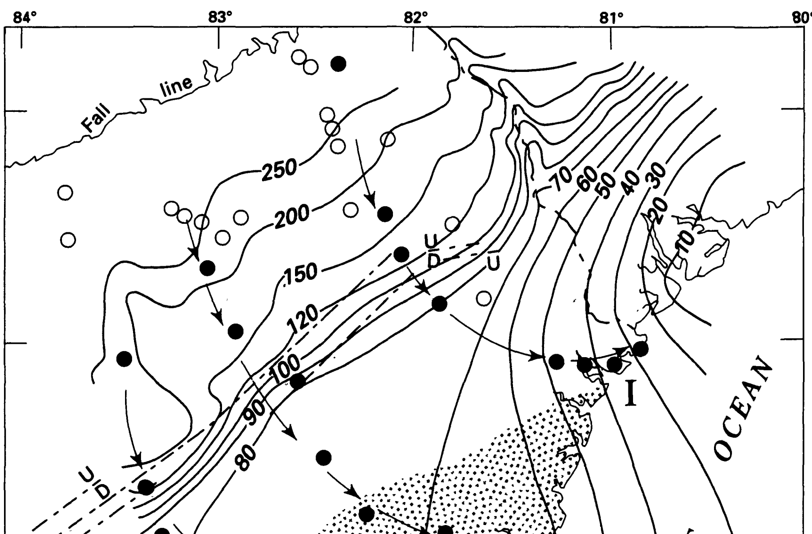

Fig. 1. Map showing locations of wells in the Upper Floridan aquifer (solid circles) and adjacent aquifers (open circles) on flow paths I through III, altitude of the predevelopment potentiometric surface of the Upper Floridan aquifer (in feet from sea level), and the zone of chloride enrichment in the Upper Floridan aquifer in southeast Georgia (pattern dotted where dissolved-chloride concentration exceeds 10 mg liter^{-1}). Northeast-trending dashed lines show the up (U) and down (D) sides of the Gulf Trough graben.

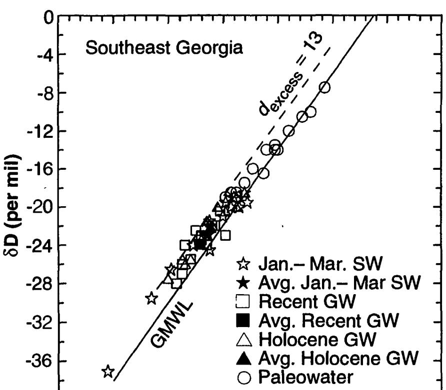

Fig. 2. A $\delta^{18}O$-δD plot showing similarities in the stable isotopic composition of winter-spring precipitation [surface waters (SW)], recent ground water (GW) with ^{14}C contents greater than 50 pmc, and Holocene ground waters with ^{14}C contents of 10 to 50 pmc. Solid symbols are average values. Paleowaters in the Floridan aquifer downgradient of the Gulf Trough are isotopically enriched relative to Holocene waters. The deuterium excess is approximately 10 to 13 per mil in the Holocene and paleowaters.

downgradient. Beyond 100 km, the patterns diverge; the increase is greatest for the southernmost flow path (flow path III) (Fig. 1). On flow paths II and III, the maximum increase is at about 180 to 200 km downgradient. The isotope shift is also observed in the Lower Floridan aquifer at the end of flow path III and in paleowaters in the Floridan aquifer system in Florida (*32*). The paleowaters plot along the GMWL with a d_{excess} similar to the recent and Holocene waters (Fig. 2); therefore, the enrichment in $\delta^{18}O$ cannot be attributed to evaporation or isotopic exchange with the rock matrix. The maximum enrichments in $\delta^{18}O$ of the Upper Floridan aquifer between the average Holocene recharge water and paleowaters from north to south along flow paths I to III are 0.7, 1.4, and 2.3 per mil, respectively (Fig. 3).

The adjusted ^{14}C data (*33*) confirm that LGM paleowaters are present in the Upper Floridan aquifer downgradient of the Gulf Trough structure. The two waters showing greatest enrichment in $\delta^{18}O$ on flow path III have adjusted radiocarbon ages of 26 ka, and the water on flow path II showing peak enrichment is dated at 24 ka (Fig. 3). The plateau in stable isotope enrichment on flow path I has an adjusted radiocarbon age of 20 ka and occurs at about the same distance downgradient as the peak enrichments found on flow paths II and III (*34*). The peak in maximum enrichment in stable isotopes may correspond to the LGM, which probably occurred about 18,000 (^{14}C) years ago.

Dissolved nitrogen and argon in Holocene ground waters and paleowaters from

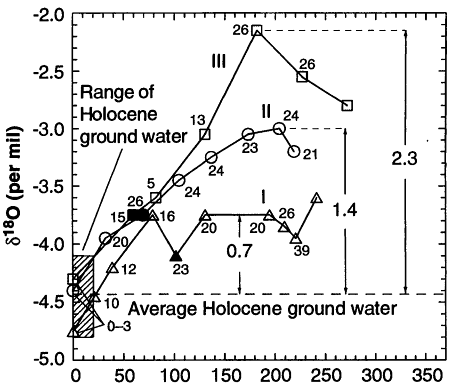

Fig. 3. Variations in $\delta^{18}O$ in Upper Floridan aquifer waters as a function of distance from recharge area on flow paths I through III. Solid points denote position of the Gulf Trough on each flow path. Maximum enrichments in $\delta^{18}O$ relative to the average Holocene ground water in southeast Georgia are 0.7, 1.4, and 2.3 per mil on flow paths I, II, and III, respectively. Numbers adjacent to sample points are adjusted radiocarbon ages in thousands of years (*33*, *34*).

southeast Georgia (*35*) indicate that recharge temperatures during the late Wisconsin averaged 5.3°C less than those of today (*36*). The paleowaters contain 2 to 4 cm^3 of excess air per liter, which is similar to that of Holocene infiltration waters (*37*).

Rayleigh model calculations of the isotopic composition of precipitation originating in low-latitude oceans, where temperature variations are small, and condensing over colder, high-latitude regions indicate that the latitudinal temperature effects between 0° and 20°C, $d\delta^{18}O/dT$ and $d\delta D/dT$, are $0.72 - 0.010T$ and $6.0 - 0.09T$ (in per mil per degree Celsius), where T is the condensation temperature in degrees Celsius (*9*). Much of the stable-isotope data for precipitation over central Europe have been correlated to latitudinal, yearly average ground-level air temperatures between 0° to 18°C (*38*) and explained by stable-isotope temperature coefficients, $d\delta^{18}O/dT$ and $d\delta D/dT$, of 0.56 ± 0.09 and 4.9 ± 0.6 per mil per degree Celsius (*9*). Smaller seasonal changes in $\delta^{18}O$ and δD result because of seasonal changes in condensation temperature and average temperature in the source area (*9*). For example, seasonal variations in $\delta^{18}O$ today in southeast Georgia are around 0.13 per mil per degree Celsius.

If we apply the $\delta^{18}O$ stable isotope temperature coefficient of 0.56 per mil per degree Celsius (9) directly to the $\delta^{18}O$ enrichment in the paleowaters from southeast Georgia and account for the oceanic (ice volume) enrichment of 1.3 per mil (*26*), air temperatures during the recharge season were nearly 2°C warmer for flow path III during the LGM than today. However, an average cooling of at least 5.3°C is indicated by the dissolved gas data and should have completely obscured the oceanic enrichment of 1.3 per mil at the LGM, resulting in stable isotope depletion or little discernible difference in stable isotopic composition between Holocene waters and LGM waters. Because the southeast-Georgia LGM waters have higher D/H and $^{18}O/^{16}O$ ratios, additional processes must have occurred that influenced the stable isotopic composition of these waters.

A change of recharge season from the present late winter-spring to summer accompanying latitudinal cooling is probably necessary but not sufficient to fully account for the observations in southeast Georgia. We demonstrated this by examining the implied paleo-seasonal variation in $\delta^{18}O$, which, for this case, should be similar to today. Today, seasonal variations in $\delta^{18}O$ of precipitation in southeast Georgia average not more than 2 per mil between winter and summer. If we assume that the most enriched water on flow path III is representative of summer precipitation in southeast Georgia at the LGM ($\delta^{18}O = -2.1$ per mil) and allow for an enrichment of 1.3 per mil in oceanic source waters, a 5.3°C cooling (in both summer and winter temperatures) indicates winter precipitation was depleted by about 1.7 per mil in $\delta^{18}O$ relative to today (paleowinter $\delta^{18}O$ in precipitation = -6.1 per mil). This indicates a seasonal variation of nearly 4 per mil in $\delta^{18}O$ during the LGM, which is at least twice that of today. Therefore, change of recharge season with latitudinal cooling is insufficient to entirely account for the observed changes in recharge temperature and stable isotope data.

Precipitation from late summer warm-core storm systems, such as hurricanes and other tropical cyclones, will likely be enriched in ^{18}O and D relative to precipitation from cold-core extratropical cyclones. Although there are no data on the occurrence of hurricanes during the LGM, climate modeling indicates that summer equatorial and Gulf of Mexico ocean surface temperatures were similar to or even slightly warmer than today (*15–18*), with Atlantic summer cyclone activity displaced southward (*39*). It is suggested that the initial stages of overland precipitation from (summer) hurricanes and tropical cyclones could provide isotopically enriched precipitation in coastal areas of the southeast United States. The precipitation pattern may be similar to that seen in the eastern end of the Sahelo-Sudanese zone of Africa today, where isotopically enriched precipitation falling at Addis Ababa, Ethiopia, may represent the early stages of moisture from monsoons arriving from the Indian Ocean (*40*).

Although sea-surface temperatures in the Gulf of Mexico were little changed during the LGM (*15–18*), surface air temperatures in the southeast United States were significantly cooler (*13*, *14*), establishing a strong continental cooling gradient northward. The differences in the magnitudes of the stable isotope enrichments along flow paths I through III may provide a maximum estimate of the continental temperature gradient at the LGM in southeast Georgia. Application of the stable isotope temperature coefficient, $\Delta\delta^{18}O/\Delta T$, of 0.56 per mil per degree Celsius to the maximum stable isotope enrichments on flow paths I to III, which have recharge areas separated by about 2° of latitude, indicates a maximum continental cooling gradient of 1.4°C per degree of latitude in southeast Georgia. This estimate may be exaggerated because intense rainfall is often associated with stable isotope depletion (amount effect) (*8*). The maximum continental temperature gradient can be compared with Atlantic sea-surface temperature gradients, which should be moderated by the Gulf Stream near the southeast Georgia coast, at the

LGM of 0.55° (February) to 0.43°C per degree of latitude (August) (*41*).

Stable isotope shifts and changes in paleorecharge temperatures can independently provide information about past temperature changes, and inconsistencies in these data provide a means of recognizing changes in other climatic variables such as moisture transport mechanisms, storm trajectories, precipitation intensity, and recharge season. In southeast Georgia, the inconsistency in stable isotope data and paleorecharge temperatures indicates significant changes in moisture transport mechanism and recharge season during the LGM.

REFERENCES AND NOTES

1. A. H. Bath, W. M. Edmunds, J. N. Andrews, in *Isotope Hydrology 1978* (International Atomic Energy Agency, Vienna, 1979), vol. II, pp. 545–566.
2. B. Blavoux and P. Olive, *J. Hydrol.* **54**, 167 (1981); J. Rudolph, H. K. Rath, C. Sonntag, in *Isotope Hydrology 1983* (International Atomic Energy Agency, Vienna, 1984), pp. 467–477; C. J. Yapp, *J. Hydrol.* **76**, 63 (1985); H. C. Claassen, *Chem. Geol.* **58**, 311 (1986); W. Richter, *Isotopenpraxis* **23**, 385 (1987); A. R. Dutton and W. W. Simpkins, *Geology* **17**, 653 (1989).
3. K. Rozanski, *Chem. Geol.* **52**, 349 (1985).
4. T. H. E. Heaton, A. S. Talma, J. C. Vogel, *Quat. Res.* **25**, 79 (1986).
5. F. M. Phillips, L. A. Peeters, M. K. Tansey, S. N. Davis, *ibid.* **26**, 179 (1986).
6. D. I. Siegel and R. J. Mandle, *ibid.* **22**, 329 (1984).
7. M. Stute and J. Deak, *Radiocarbon* **31**, 902 (1989); M. Stute and C. Sonntag, in *Isotopes of Noble Gases as Tracers in Environmental Studies* (International Atomic Energy Agency, Vienna, 1992), pp. 111–122; M. Stute and P. Schlosser, in *Climate Change in Continental Isotopic Records*, P. K. Smart, K. C. Lohmann, J. McKenzie, S. Savin, Eds. (*Geophys. Monogr. 78*, American Geophysical Union, Washington, DC, 1993), pp. 89–100.
8. W. Dansgaard, *Tellus* **16**, 436 (1964); S. Joussaume, J. Jouzel, R. Sadoury, *Nature* **311**, 24 (1984); K. Rozanski, L. Araguás-Araguás, R. Gonfiantini, *Science* **258**, 981 (1992); in *Climate Change in Continental Isotopic Records*, P. K. Swart, K. C. Lohmann, J. McKenzie, S. Savin, Eds. (*Geophys. Monogr. 78*, American Geophysical Union, Washington, DC, 1993), pp. 1–36.
9. C. M. van der Straaten and W. G. Mook, in *Palaeoclimates and Palaeowaters: A Collection of Environmental Isotope Studies* (International Atomic Energy Agency, Vienna, 1983), pp. 53–64.
10. D. M. Ferree, S. Christenson, A. H. Rea, B. A. Mesander, *U.S. Geol. Surv. Open-File Rep. 92-641* (1992); D. L. Parkhurst, S. Christenson, G. N. Breit, *U.S. Geol. Surv. Open-File Rep. 92-642*, in press. A maximum depletion of 1.5 per mil in $\delta^{18}O$ relative to Holocene ground waters combined with an enrichment of 1.3 per mil in ocean source waters at the LGM and a $\delta^{18}O$ temperature coefficient of 0.56 per mil per degree Celsius indicates a 5°C cooling in central Oklahoma.
11. L. Benson and H. Klieforth, in *Aspects of Climate Variability in the Pacific and the Western Americas*, D. H. Peterson, Ed. (*Geophys. Monogr. 55*, American Geophysical Union, Washington, DC, 1989), pp. 41–59.
12. M. Stute, P. Schlosser, J. F. Clark, W. S. Broecker, *Science* **256**, 1000 (1992).
13. W. A. Watts, *Quat. Res.* **13**, 187 (1980).
14. D. W. Woodcock and P. V. Wells, *Palaeogeogr. Palaeoclimatol. Palaeoecol.* **79**, 305 (1990).
15. CLIMAP Project Members, *Science* **191**, 1131 (1976); *Geol. Soc. Am. Map Chart Ser. MC-36* (1981); W. L. Gates, *Science* **191**, 1138 (1976); W. L. Gates, *J. Atmos. Sci.* **33**, 1844 (1976).
16. J. E. Kutzbach, in *North America and Adjacent Oceans at Last Deglaciation*, vol. K3 of *The Geology of North America*, W. F. Ruddiman and H. E. Wright Jr., Eds. (Geological Society of America, Boulder, CO, 1987), pp. 425–446.
17. J. E. Kutzbach and H. E. Wright Jr., *Quat. Sci. Rev.* **4**, 147 (1985).
18. D. Rind and D. Peteet, *Quat. Res.* **24**, 1 (1985); T. Webb III, P. J. Bartlein, J. E. Kutzbach, in (*16*), pp. 447–462; H. E. Wright Jr., *ibid.*, pp. 479–488.
19. R. G. Barry, in *The Late Pleistocene*, vol. 1 of *Late-Quaternary Environments of the United States*, S. C. Porter, Ed. (Univ. of Minnesota Press, Minneapolis, MN, 1983), pp. 390–407; W. A. Watts, *ibid.*, pp. 294–310.
20. J. Ch. Fontes, M. Stute, P. Schlosser, W. S. Broecker, *Eos* **74**, 21 (1993).
21. V. T. Stringfield, *U.S. Geol. Surv. Prof. Pap. 517* (1966); W. Back and B. B. Hanshaw, *J. Hydrol.* **10**, 330 (1970); W. R. Aucott, *U.S. Geol. Surv. Water Resour. Invest. Rep. 88-4057* (1988); R. H. Johnston and P. W. Bush, *U.S. Geol. Surv. Prof. Pap. 1403-A* (1988); R. E. Krause and R. B. Randolph, *U.S. Geol. Surv. Prof. Pap. 1403-D* (1989); M. L. Maslia and L. R. Hayes, *U.S. Geol. Surv. Prof. Pap. 1403-H* (1988); J. A. Miller, *U.S. Geol. Surv. Prof. Pap. 1403-B* (1986); L. N. Plummer, *Water Resour. Res.* 13, 801 (1977); ———, D. L. Parkhurst, D. C. Thorstenson, *Geochim. Cosmochim. Acta* **47**, 665 (1983); C. L. Sprinkle, *U.S. Geol. Surv. Prof. Pap. 1403-I* (1989); J. A. Miller, *U.S. Geol. Surv. Hydrol. Invest. Atlas 730-G* (1990); B. G. Katz, *U.S. Geol. Surv. Water Resour. Invest. Rep. 91-4196* (1992).
22. A. Swancar and C. B. Hutchinson, *U.S. Geol. Surv. Open-File Rep. 92-47* (1992).
23. P. W. Bush and R. H. Johnston, *U.S. Geol. Surv. Prof. Pap. 1403-C* (1988).
24. J. A. Miller and R. A. Renken, *U.S. Geol. Surv. Water Resour. Invest. Rep. 87-4202* (1988).
25. Hydraulic gradients were calculated along flow paths I through III between points immediately downgradient of the Gulf Trough and the Atlantic Coast with the predevelopment potentiometric surface (Fig. 1). The hydraulic conductivity and effective porosity were 0.0007 m s^{-1} and 0.3, respectively (*21, 22*).
26. N. J. Shackleton, *Quat. Sci. Rev.* **6**, 183 (1987); R. G. Fairbanks, *Nature* **342**, 637 (1989).
27. T. J. Hughes *et al.*, in *The Last Great Ice Sheets*, G. H. Denton and T. J. Hughes, Eds. (Wiley, New York, 1981), pp. 263–317; A. L. Bloom, in (*19*), pp. 215–229.
28. Dissolved chloride concentrations are typically 10 to 50 mg L^{-1} in a broad zone downgradient of the Gulf Trough (Fig. 1) and locally reach several thousand milligrams per liter in coastal areas (only). Upgradient of the zone of chloride enrichment and to the north over most of flow path I, chloride concentrations are typically 2 to 5 mg $liter^{-1}$, similar to the chloride content of recent recharge waters. The Br/Cl ratios are similar to those of seawater throughout southeast Georgia. In addition to an increase in diffuse upward leakage from the Lower Floridan aquifer during the LGM, several other processes may have contributed dissolved chloride to the paleowaters: (i) incomplete flushing of paleoseawater; (ii) seawater intrusion (coastal zones only) in populated areas caused by lowered freshwater heads from ground-water withdrawals near Savannah and Brunswick, Georgia, and Jacksonville, Florida; and (iii) chloride enrichment in paleorecharge waters as a result of lower recharge rates in a drier climate. Lowered sea level usually causes a decrease in dissolved chloride content of ground water because of greater distances between the oceans and recharge areas (*1, 2, 42*); however, drier conditions in the southeast United States at the LGM (*19*) suggest lowered recharge rates. The dissolved chloride data for southeast Georgia are not inconsistent with a significant reduction in recharge rate or an increased rate of dry deposition during the late Wisconsin.
29. All stable isotope measurements were determined by the U.S. Geological Survey (USGS) Stable Isotope Laboratory, Reston, Virginia. The stable isotope results are reported in per mil relative to VSMOW (Vienna Standard Mean Ocean Water) and normalized (*43*) on scales such that the oxygen and hydrogen isotopic values of SLAP (Standard Light Antartic Precipitation) are −55.5 and −428 per mil, respectively. The 2σ precision of oxygen and hydrogen isotope results is 0.2 and 1.5 per mil, respectively.
30. Surface waters collected from USGS monitoring stations during 1985–87. T. B. Coplen and C. Kendall, unpublished data.
31. The average air temperature for January to April, corresponding to the recharge season for southeast Georgia, over the past 100 years of record (*44*) is 14.7°C. The average $\delta^{18}O$ and δD compositions of 13 Holocene ground waters in southeast Georgia are -4.43 ± 0.29 per mil and -23.9 ± 2.2 per mil, respectively. Fifteen surface water samples from USGS National Stream Quality Accounting Network (NASQAN) surface water monitoring stations in south-central Georgia collected between January and March of 1985–87 average -4.3 ± 0.7 per mil in $\delta^{18}O$ and -22.9 ± 4.9 per mil in δD.
32. Stable isotope enrichment occurs at 600 m in the Lower Floridan aquifer at the end of flow path III (Fig. 1) where the $\delta^{18}O$ of water from the freshwater–saltwater interface (44.4% seawater on the basis of chloride content) is −1.5 per mil. If the $\delta^{18}O$ of the seawater component is 0 per mil, the $\delta^{18}O$ of the freshwater fraction of this Lower Floridan sample is −2.7 per mil, which is comparable to −2.8 per mil measured in the Upper Floridan aquifer at a total depth of 274 m (Fig. 1) at this locality. Paleowaters in confined portions of the Floridan aquifer of central Florida plotting on the GMWL are enriched from 1.2 to 1.9 per mil in $\delta^{18}O$ relative to Holocene ground water (*22, 45*). Other paleowaters in confined portions of the Floridan aquifer in central Florida show even greater enrichment in $\delta^{18}O$ and plot along an evaporation trend relative to the GMWL (*45*).
33. The ^{14}C content of the dissolved inorganic carbon varies from 107 pmc for some recent ground waters to 0.12 ± 0.1 pmc for water near the end of flow path I. Most of the waters downgradient of the Gulf Trough contain less than 2 pmc, except for flow path III, which contains as much as 17 pmc immediately downgradient of the Gulf Trough in an area of incomplete confinement. Precise assignment of radiocarbon ages depends on knowledge of the ^{14}C content of the recharge water and adjustment for the mineral-water reactions along the flow path that alter the ^{14}C concentration of the dissolved inorganic carbon. A Tamers model was applied to the initial (confined) water on each Upper Floridan aquifer flow path in southeast Georgia to estimate the initial ^{14}C value. A geochemical mass balance reaction model was constructed along the flow path and used to adjust the initial ^{14}C value for reactions as in (*46*). The predominant reactions considered are dissolution of dolomite and anhydrite, precipitation of calcite, oxidation of organic matter coupled with microbially mediated sulfate reduction, iron reduction and pyrite precipitation, calcium-sodium ion exchange, and carbon isotope exchange accompanying the recrystallization of calcite. Reaction models were found that reproduced the observed ^{13}C of dissolved inorganic carbon. Some of the modeled ages are more reliable than others owing to the magnitude of the reaction corrections and the uncertainties in the ^{14}C measurements. All adjusted radiocarbon ages are given on Fig. 3 and have estimated uncertainties of ±5 ka.
34. Because recharge rates, hydraulic gradients, and travel times have probably varied significantly in the past, water age cannot be directly related to distance of flow on a given flow path. It can only be assumed that water age increases with distance. Most water in the Floridan aquifer downgradient of the Gulf Trough has an adjusted radiocarbon age in excess of 20 ka. The abundance of adjusted radiocarbon ages between 20 and 26 ka downgradient of the Gulf Trough may

have resulted from expected increased flow velocities in response to a lowering of sea level. Upgradient of the Gulf Trough, most waters have adjusted radiocarbon ages greater than 10 ka, suggesting little recent (past 10 ka) recharge.

35. The recharge temperature refers to the temperature at the base of the unsaturated zone during ground-water recharge. It is assumed that water infiltrating the unsaturated zone maintains equilibrium with the unsaturated zone air, and as further recharge occurs, the infiltration water becomes isolated from further exchange with the unsaturated-zone air (*4, 7, 47*). Recharge temperatures were determined by gas chromatographic analyses of dissolved nitrogen and argon (*4, 47*) and have a precision of ±1°C. Overall uncertainties in N_2/Ar recharge temperatures are near ±2°C, considering uncertainties in amounts of excess air and denitrification.
36. The average recharge temperature, determined from dissolved nitrogen and argon analyses, of 22 Holocene ground waters from southeast Georgia (*37*) is 15.2° ± 1.6°C, and that of 21 paleowaters is 9.9° ± 1.9°C. The mean annual temperature today is approximately 19°C (*44*). Recent calibration measurements completed after acceptance of this paper indicate that recharge temperatures determined by our nitrogen-argon gas chromatographic system should be warmer by approximately 3.1° ± 1.6°C. This correction places the Holocene recharge temperatures near the expected mean annual temperature. Because the error applies to both Holocene and paleowaters, the average cooling of 5.3°C in paleorecharge temperatures is retained.
37. Most of the Holocene waters are from two recharge areas to the Upper Floridan aquifer in south-central Georgia (flow path III): (i) near Valdosta, Georgia (waters with low excess-air content caused by direct recharge from a river through sinkholes), and (ii) near Albany, Georgia (waters with 2 to 5 cm^3 of excess air per liter that are recharged by infiltration through a shallow unsaturated zone). Several other Holocene waters are from the recharge areas on flow paths I and II. All paleowaters are from flow paths I and II.
38. Ground-level air temperatures may be several degrees warmer than temperatures at the base of clouds; however, the slope of stable isotope variations with temperature should be unaffected by this difference (*9*).
39. J. Williams, R. G. Barry, W. M. Washington, *J. Appl. Meteorol.* **13**, 305 (1974).
40. A. Joseph, J. P. Frangi, J. F. Aranyossy, *J. Geophys. Res.* **97**, 7543 (1992).
41. J. Imbrie, A. McIntyre, T. C. Moore Jr., in (*19*), pp. 230–236.
42. P. L. Airey *et al.*, in (*1*), vol. I, pp. 205–219; M. R. Davidson and P. L. Airey, *J. Hydrol.* **58**, 131 (1982); C. B. Purdy, G. S. Burr, M. Rubin, G. R. Helz, A. C. Mignerey, *Radiocarbon* **34**, 654 (1992).
43. T. B. Coplen, *Chem. Geol.* **72**, 293 (1988).
44. T. R. Karl, C. N. Williams, F. T. Quinlan, T. A. Boden, *United States Climatology Network (HCN) Serial Temperature and Precipitation Data* (*Environ. Sci. Publ. 3404*, Oak Ridge National Laboratory, Oak Ridge, TN, 1990).
45. L. N. Plummer and C. L. Sprinkle, unpublished data.
46. L. N. Plummer, E. C. Prestemon, D. L. Parkhurst, *U.S. Geol. Surv. Water Resour. Invest. Rep. 91-4078* (1991).
47. T. H. E. Heaton, *Trans. Geol. Soc. S. Afr.* **84**, 91 (1981); ——— and J. C. Vogel, *J. Hydrol.* **50**, 201 (1981).
48. I have benefited from discussions with T. B. Coplen and I. J. Winograd and comments from L. V. Benson, H. C. Claassen, T. B. Coplen, M. Stute, P. Schlosser, I. J. Winograd, and an anonymous reviewer. T. B. Coplen and C. Kendall provided unpublished stable isotope data for surface waters in southeast Georgia. J. F. Clark assisted in collecting water samples for dissolved nitrogen and argon content. Other chemical and isotopic data used in this report were collected with the assistance of E. Busenberg, S. A. Longsworth, and C. L. Sprinkle.

14 July 1993; accepted 15 October 1993

Evidence of the Growth Plate and the Growth of Long Bones in Juvenile Dinosaurs

Claudia Barreto,* Ralph M. Albrecht, Dale E. Bjorling, John R. Horner, Norman J. Wilsman

Histological and ultrastructural evaluation of the ends of long bones of juvenile dinosaurs from the Upper Cretaceous Two Medicine Formation of Montana revealed the preservation of growth plates. Growth plates are discs of cartilage present near the ends of growing long bones that generate bone elongation. Comparison of the fossils with modern taxa demonstrated homology of the growth plate in birds and dinosaurs. The presence of an avian-type growth plate in dinosaurs adds a shared derived anatomical character corroborating inclusion of birds within the Dinosauria. Additionally, possession of a growth plate, which in birds is capable of producing rapid determinate long bone growth, implies that an avian developmental pattern may have been present in these dinosaurs.

In adolescent animals, growth plate cartilage, present near the ends of long bones, is responsible for producing bone growth (Fig. 1). The cells of the growth plate (chondrocytes) have a particular temporal and spatial arrangement and undergo a series of morphologic and other phenotypic changes in their brief life history. Germinal chondrocytes at the articular end of the growth plate enter the cell cycle and proliferate. After leaving the cell cycle, differentiated chondrocytes mature and hypertrophy. Growth plate chondrocytes produce and maintain a specialized extracellular matrix, and each chondrocyte is thus enclosed in a lacuna. The chemical composition of the extracellular matrix is critical to chondrocytic development and proper function of the growth plate (*1*). At the metaphyseal end of the growth plate, endochondral ossification occurs. Here hypertrophic chondrocytes calcify their surrounding matrix and die at the junction of the cartilaginous growth plate with the bony metaphysis (chondro-osseous junction). With chondrocytic death, blood vessels, osteoclasts, and osteoblasts (bone-forming cells) invade the space formerly occupied by the chondrocytes. The osteoblasts then use the calcified cartilage matrix as a scaffold on which to produce new bone, thereby adding to the length of the bone shaft.

Growth plate morphology, such as growth plate height and chondrocytic volumes and shapes, varies among species, within a species at different ages, and even within a bone in which the ends grow at different rates. The mechanisms by which these morphological differences are translated into differential rates of growth are beginning to be understood (*2*). Among living animals, the avian growth plate has a distinct organization, most notably in the shape of the chondro-osseous junction. This morphology may reflect a unique strategy for rapid bone elongation in which metaphyseal bone production is minimized.

Direct observation of the biology of extinct species is not possible, and therefore, our understanding of dinosaur growth is limited. While soft tissue, including cartilage, is rarely preserved in the fossil record, the calcified hypertrophic zone of the growth plate, adjacent to the newly forming bone, has greater potential to become fossilized. Because growth plate morphology can be related to rate of bone growth, comparison of the histologic appearance of the dinosaur growth plate with that of living animals may provide understanding of long bone growth processes in dinosaurs. We studied the microscopic morphology of growth plates at the ends of juvenile long bones of the dinosaur *Maiasaura* (Ornithischia: Hadrosauridae), a bipedal, duck-billed dinosaur (*3*), and compared the microscopic structure with the growth plates of a bird (chicken), a mammal (dog), and an ectothermic reptile (monitor lizard). Birds and lizards have evolved from ancestors classified as diapsid reptiles, whereas mammalian ancestors are synapsid reptiles (*4*).

Maiasaura was abundant in North America in the Late Cretaceous Period. The adults reached lengths of 9 m. The *Maiasaura* specimens that we studied were recovered from the Two Medicine Forma-

C. Barreto, D. E. Bjorling, N. J. Wilsman, School of Veterinary Medicine, University of Wisconsin, Madison, WI 53706.
R. M. Albrecht, Department of Animal Health and Biomedical Sciences, University of Wisconsin, Madison, WI 53706.
J. R. Horner, Museum of the Rockies, Montana State University, Bozeman, MT 59717.

*To whom correspondence should be addressed.